

## Heat Loss Prediction from Solar LFR Linear Evacuated Surface Receiver with Variable 2-Stage Concentrated Flux

K. S. Reddy<sup>1\*</sup>, Shanmugapriya Balaji<sup>1</sup>, T. Sundararajan<sup>2</sup>

<sup>1</sup>Heat Transfer and Thermal Power Laboratory,

<sup>2</sup>Thermodynamics and Combustion Engineering Laboratory

Department of Mechanical Engineering

Indian Institute of Technology Madras, Chennai – 600036, India

\*Corresponding Author, Email:ksreddy@iitm.ac.in

### Abstract

A numerical study has been carried out to analyse the thermal performance of the receiver system of solar Linear Fresnel Reflector (LFR) module. Realistic flux conditions obtained by the optical analyses are applied as the boundary condition to the circumference of the absorber. Heat losses caused by convection as well as radiation from the parabolic secondary receiver are investigated under evacuated and non-evacuated annular region between the absorber and the glass tube. The investigation has been carried out to determine the heat loss by varying the annular gap between the absorber tube and the protective glass.

*Keywords: Solar flux, variable flux distribution, evacuated, non-evacuated condition*

---

### 1. Introduction

A progressive method observed is the Linear Fresnel reflector (LFR) technology to harness the solar energy for power and thermal needs of the society. An LFR system consists of the primary mirror strips in conjunction with the uniaxial tracking system, receiver system comprising a glass tube enclosing the absorber with a secondary reflector. The receiver system of solar Linear Fresnel Reflector (LFR) module plays a vital part in the conversion of the solar rays to thermal energy (Reddy and Kumar, 2014), (Singh et al., 2010)) and the schematic of the LFR is shown in Fig. 1(a). The present work has been carried out based on the study carried by peers on a wide range of collectors. Zou et al., 2017 comprehensively studied the optical performance of parabolic trough collector based on Monte Carlo Ray Tracing method (MCRT) and theoretical method. The angle span of each flux distribution region was derived theoretically, and the variations of those parameters with different geometrical configurations were displayed. Geometrical parameters such as aperture width, focal length and absorber diameter had a greater influence on the performance of the system. It was concluded that the absorber diameter had to be larger than the spot size of the reflected light cone on the absorber to avoid rays escaping which can cause great optical loss. Guadamud et al., 2015 modelled an LFR with a parallel modular object-oriented methodology which considered the elements of the receiver system namely the insulation material, glass cover, tube, pipe, etc. The global model is composed of 4 submodels -heat conduction, two/single-phase flow, thermal radiation and natural convection. It was found that the CFD&HT simulations using LES modelling allowed more realistic results. Chaitanya Prasad et al., 2017 used the variable aim lines for primary mirrors to defocus and spread the radiation flux in a more uniform manner over the absorber. Both the tilt angles and the radii of curvature of the individual Fresnel mirrors are modified to obtain a better flux uniformity. With the variable aim line concept high optical efficiency of 76.4% and a coefficient of flux variation value of 0.13 were obtained. On the other hand, 74.9% and 70.9% of optical efficiencies along with 0.17 and 0.33 values of coefficient of variation were obtained with compound parabolic concentrator and trapezoidal concentrator profiles respectively. Okafor et al., 2017, 2014 carried out a numerical study on the influence of circumferential uniform and non-uniform solar heat flux distributions on the internal and overall heat transfer coefficients of the absorber tubes of a linear Fresnel solar collector was investigated. A 3D steady-state numerical simulation was implemented based on ANSYS Fluent code version 14. The non-uniform solar heat flux distribution was modelled as a sinusoidal function of the concentrated solar heat flux incident on the circumference of the absorber tube. The k-e model was used to study the turbulent flow of the heat transfer fluid through the absorber tube. Hence it is clear that study of modelling and the heat loss analysis from the receiver system becomes crucial to determine the efficiency of the system. In the present heat loss analysis, circumferential non-uniform heat flux distribution on the outer wall of the absorber tube is considered. Investigation of non-

uniform flux distribution around the absorber is the more practical way of analysis compared to the constant flux conditions carried out by the peers. In the present work the investigation is carried for two cases: First, the annular area between the absorber tube and the protective glass tube is considered to be in the non-evacuated state and secondly, in the evacuated state. Heat losses in the convection and radiation mode are analysed for different flux conditions. Investigation on the heat loss dependent on the annular gap between the absorber and the protective glass tube are studied. Initial work deals with the optical distribution of the flux and the distribution have been homogenised with the parabolic profiled secondary reflector (Balaji et al., 2016). The variable distribution around the absorber is shown in Fig. 1(b).

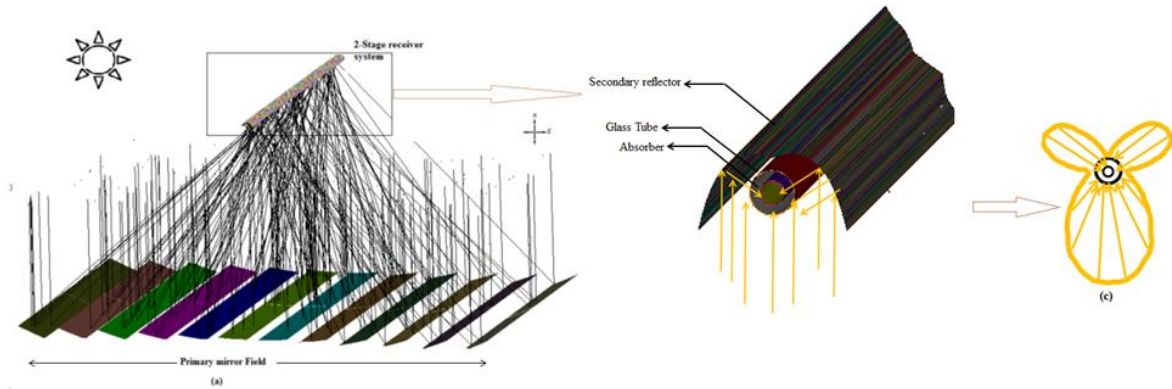


Fig. 1: (a) Schematic representation of Linear Fresnel Concentrator with secondary reflector (b) 2-Stage reflector system with solar ray (c) variable flux distribution around absorber

## 2. Description of LFR system

The Linear Fresnel Reflector/Concentrator(LFR) consists of an array of twelve long, parallel mirrors. The primary mirrors are tilted suitably and are equipped with one-dimensional tracking such that the solar rays from each mirror can be focused on one or more number of absorbers. An evacuated glass cover surrounds the absorber to prevent convective heat losses to the atmosphere. In the absence of the evacuated glass cover, the aperture opening of the secondary reflector covered by a glass pane. The absorber with the glass cover is mounted inside the secondary reflector module. Parameters of the pilot plant developed in Vallipuram (12.65N, 79.74E), Tamil Nadu, India is considered for the comprehensive study. The LFR system consists of a storage-integrated solar collector field of approximately 125 kWth capacity with the variable steam output (50 bar pressure and 350–400 °C temperature). Twelve primary reflectors with mild parabolic curvature are managed by a single axis tracking system. An absorber tube placed inside an evacuated glass cover for the reduction of convective heat losses is placed at the focal point of the primary reflectors. A selectively coated absorber tube for higher optical emissivity is used. A secondary reflector parabolic in profile surrounds both the absorber with the glass tube. In order to improve the flux distribution along the circumference of the absorber thereby increase the concentration ratio, secondary reflectors are used. The second stage reflector maximizes the flux coverage area by re-reflecting the rays to the surface of the absorber. The 2 –stage reflector also ensures to enlarge the focused rays on the absorber thereby preventing the hot spots. Progressive analysis has been carried out to estimate the heat losses from the receiver system. Initially, the optical analysis is done to obtain an optimized flux along the circumference of the absorber and then the thermal study is performed.

## 3. Thermal Analysis

The thermal investigation is carried out for the receiver system comprising of the parabolic secondary reflector with an absorber tube placed in a glass tube. Optically optimised parameters from the earlier study namely the acceptance angle of the 2-stage reflector, truncation point on the reflector, the focal position of the absorber tube, the ratio of the gap between the reflector and the absorber to the height of the reflector are considered for the numerical study. The flux thus obtained from the optical analysis is applied as a user-defined function (UDF) in the form of a polynomial curve. The curve is a function of the angular position of the flux along the circumference of the absorber. The investigation is carried out with the different flux conditions and a parametric analysis is carried out to determine the heat loss for the different annular gap between the absorber and the glass tube. Laminar, steady state, 2D governing equations are solved in Fluent 14.5. The flow and thermal behaviours of the receiver system are considered under non-Boussinesq conditions.

### 3.1 Governing Equations

Flow and the heat transfer in the 2-stage reflectors are solved simultaneously by the mass, momentum and energy equations with Cartesian coordinates by Fluent Inc (2005). By the law of conservation of mass, the continuity equation is given by:

$$\frac{\partial(\rho_f u)}{\partial x} + \frac{\partial(\rho_f v)}{\partial y} = 0 \quad (\text{eq. 1})$$

x- y Momentum equations:

$$\rho_f \left( u \frac{\partial u}{\partial x} + v \frac{\partial u}{\partial y} \right) = - \frac{\partial P}{\partial x} + \frac{\partial}{\partial y} \left( \mu \frac{\partial u}{\partial y} \right) + \frac{\partial}{\partial x} \left( \mu \frac{\partial u}{\partial x} \right) \quad (\text{eq.2})$$

$$\rho_f \left( u \frac{\partial v}{\partial x} + v \frac{\partial v}{\partial y} \right) = - \frac{\partial P}{\partial y} + \frac{\partial}{\partial x} \left( \mu \frac{\partial v}{\partial x} \right) + \frac{\partial}{\partial y} \left( \mu \frac{\partial v}{\partial y} \right) + \rho_f g \beta (T - T_{\text{ref}}) \quad (\text{eq.3})$$

Energy equation is solved by:

$$\rho_f C_p \left( u \frac{\partial T}{\partial x} + v \frac{\partial T}{\partial y} \right) = \frac{\partial}{\partial y} \left( k_f \frac{\partial T}{\partial y} \right) + \frac{\partial}{\partial x} \left( k_f \frac{\partial T}{\partial x} \right) \quad (\text{eq.4})$$

where  $u, v$  represents the velocity components in x and y-direction respectively,  $\rho$  is the density of the air inside the cavity in  $\text{kg/m}^3$ ,  $P$  is the pressure in  $\text{N/m}^2$ ,  $k_f$  represents the thermal conductivity of the fluid in  $\text{W/mK}$ .

Surface-to-Surface (S2S) radiation model is used to model the radiation heat transfer of the secondary reflector system. This model helps to assume the receiver system in an air enclosed domain to be a non-participating medium by ignoring the emission and the scattering effects. The incident flux from the surface comprises of two components, the emitted flux and the reflected flux. Both the components of flux together constitute the radiosity ( $J_i$ ) of the surface. The radiated flux depends on the flux falling on the surface from the surrounding and it is given by (Siegel, R., Howell, 2002) as

$$q_{\text{out},i} = \varepsilon_i \sigma T_i^4 + (1 - \varepsilon_i) q_{\text{in},i} \quad (\text{eq.5})$$

Interception by the two surfaces by radiation is defined as view factor  $F_{ij}$  that is independent on the surface properties and temperature. Hence the incident flux is given by.

$$A_i q_{\text{in},i} = \sum_{j=1}^N A_j q_{\text{out},j} F_{ji} \quad (\text{eq.6})$$

Based on the reciprocity theorem

$$A_j F_{ji} = A_i F_{ij} \quad (\text{eq.7})$$

Replacing (7) in (6),

$$q_{\text{in},i} = \sum_{j=1}^N q_{\text{out},j} F_{ji} \quad (\text{eq.8})$$

$$q_{\text{out},i} = \varepsilon_i \sigma T_i^4 + (1 - \varepsilon_i) \sum_{j=1}^N F_{ij} q_{\text{out},j} \quad (\text{eq.9})$$

The sum of the reflected and the emitted fluxes, radiosity  $J_i$  is defined as the total radiation energy leaving a surface per unit time and per unit area. Hence

$$E_i = J_i - (1 - \varepsilon_i) \sum_{j=1}^N F_{ij} J_j \quad \text{where } E_i = \varepsilon_i \sigma T_i^4 \quad (\text{eq.10})$$

$$E_i = \sum_{j=1}^N (\delta_{ij} - (1 - \varepsilon_i) F_{ij}) J_j \quad \text{where } \delta_{ij} \text{ is the kronector delta given by } \delta_{ij} = \begin{cases} 1 & \text{when } i = j \\ 0 & \text{when } i \neq j \end{cases}$$

Hence the radiosity expression is given by  $E = KJ$  where  $K$  is a  $N \times N$  matrix of the form

$$K = (\delta_{ij} - (1 - \varepsilon_i) F_{ij}) \quad (\text{eq.11})$$

In the above equations,  $J$  is the radiosity vector and  $E$  is the emissive power vector.

### 3.2. Boundary conditions

The 2-stage receiver system under study is an open aperture system and all the modes of heat transfer conduction, convection and radiation re influenced by the atmospheric condition. Hence the simulation is carried out by enclosing the receiver system in a domain property is simulated with the ambient conditions of temperature and pressure. The inlet of the domain is provided with pressure inlet boundary condition and the outlet of the domain is pressure outlet conditions, while the sides of the domain are pressure inlet conditions. The absorber tube is exposed to the flux reflected by the primary mirrors and the flux re-reflected by the secondary reflectors. Hence the non-uniform flux obtained from the optical study is imbibed as the boundary condition. The non-uniform flux is applied as the user-defined function. The absorber is coated with sputtered cermet of emissivity 0.075. The coupled condition is provided as a boundary value for the glass tube with the transmissivity of 0.95. Figure 2 shows the boundary condition of the 2-stage secondary reflector.

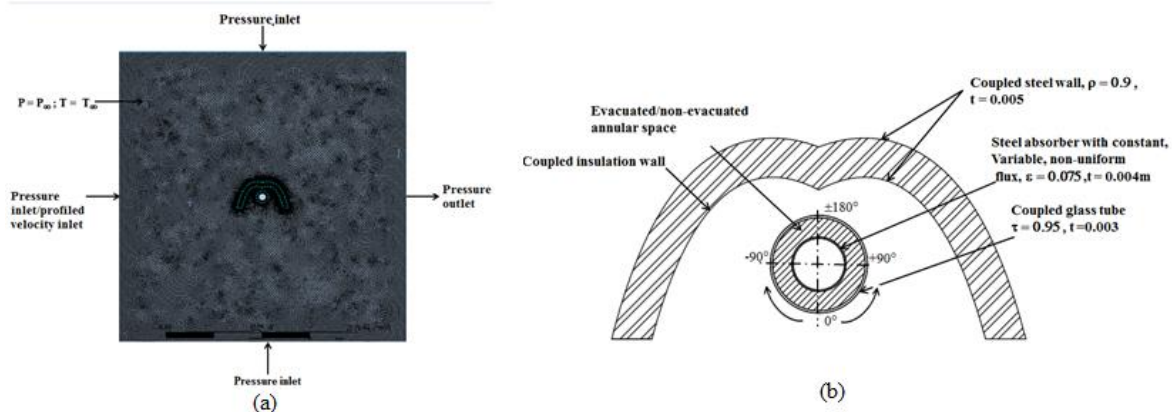


Fig. 2: Boundary condition of domain with 2-stage reflector of Linear Fresnel Concentrator (b) Boundary condition of 2-Stage reflector system

### 3.3. Boundary conditions

The size of the simulated domain is crucial since the heat loss output is dependent on it. Hence simulation is optimised by varying the inlet, side wall and the output length of the domain. Optimised domain size is assessed to be about 20D from the absorber on all the four sides. Skewness–Neighbor coupling of PSO algorithm is adopted with the convergence criterion of  $10^{-6}$  on the residuals of the continuity equation and momentum equation. Deviation observed for the grid size with elements 8, 56,178 is appreciable to proceed the simulation. Validation of the present work was done with the work carried on by Reddy and Kumar, 2014; Sahoo et al., 2012 and the deviation in the results were found to be less than 10% which is acceptable.

## 4. Results and Discussion

A parametric study has been carried out based on the direct normal irradiance (DNI) and the annular gap between the absorber and the protective glass. The annular gap is non-dimensionalized by considering the ratio of the diameter of the absorber and the diameter of the protective glass. The study has been carried out for two different conditions of the annular gap: one, when the annular gap is filled with air as the residual gas and second, considering vacuum in the annular region.

### 4.1 Effect of DNI on the heat loss from the 2-stage receiver system

Temperature contours of the parabolic secondary reflector for DNI for  $750\text{W/m}^2$  and  $1000\text{W/m}^2$  for non-evacuated and evacuated annular region are shown in Fig.3. It is observed that because of the presence of air in the annular space between the absorber tube and the protective glass tube, buoyancy effect exist in the annular space. The hot wave in the annular space move upwards and the heat transfer occurs to the entire cavity region. Plume formation apparently illustrates the heat loss to the atmosphere. Whereas when the annular region is evacuated, the heat transfer from the upper portion of the absorber spread out symmetrically on both sides of the absorber within the cavity region. As the DNI increases the temperature increases and the hot wave distributes throughout the cavity and heat losses from the aperture opening.

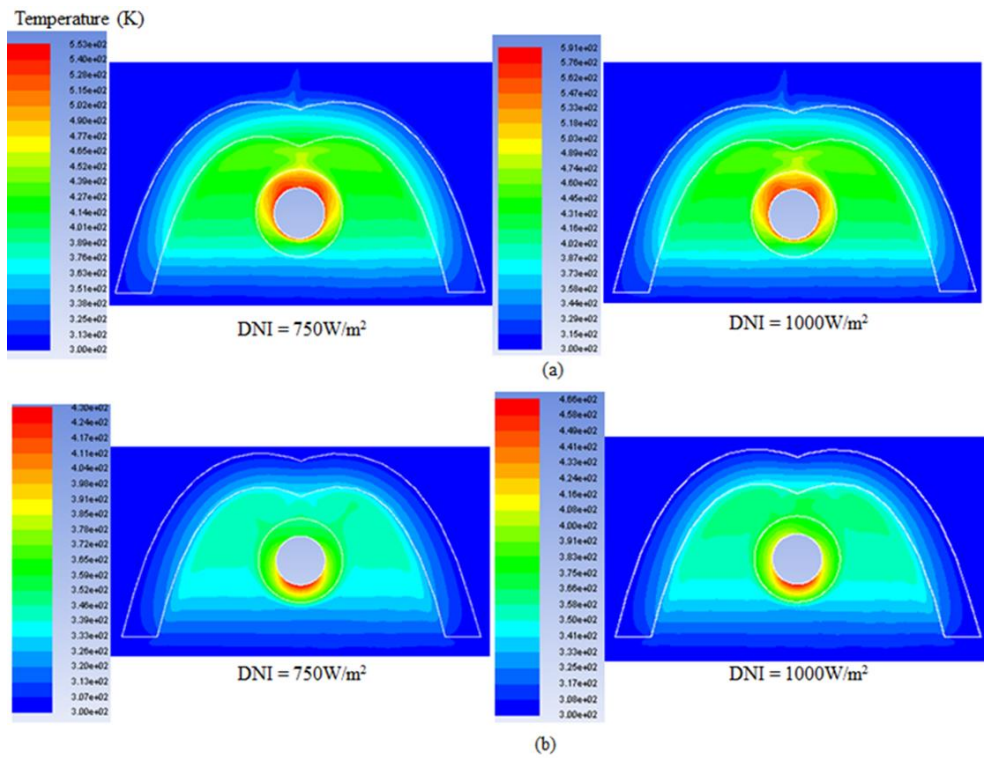


Fig. 3: Temperature contours of PB secondary reflector for different non-uniform flux distribution around the absorber tube with (a) non-evacuated annular (b) evacuated annular region

Figure 4 shows the total heat loss from the receiver system for the DNI ranging from  $250\text{W/m}^2$  to  $1000\text{W/m}^2$  under the non-evacuated condition i.e., when the annular gap is filled with air, the heat loss varies from  $47.14\text{W/m}$  to  $172\text{W/m}$  for  $250\text{W/m}^2$  to  $1000\text{W/m}^2$  respectively. When the annular region is evacuated, the percentage of heat loss is reduced from 16% to 70%. It is observed that at lower DNI, the percentage of deviation is less compared to that at higher DNI. As expected, as the DNI increases, the percentage of heat loss also increases.

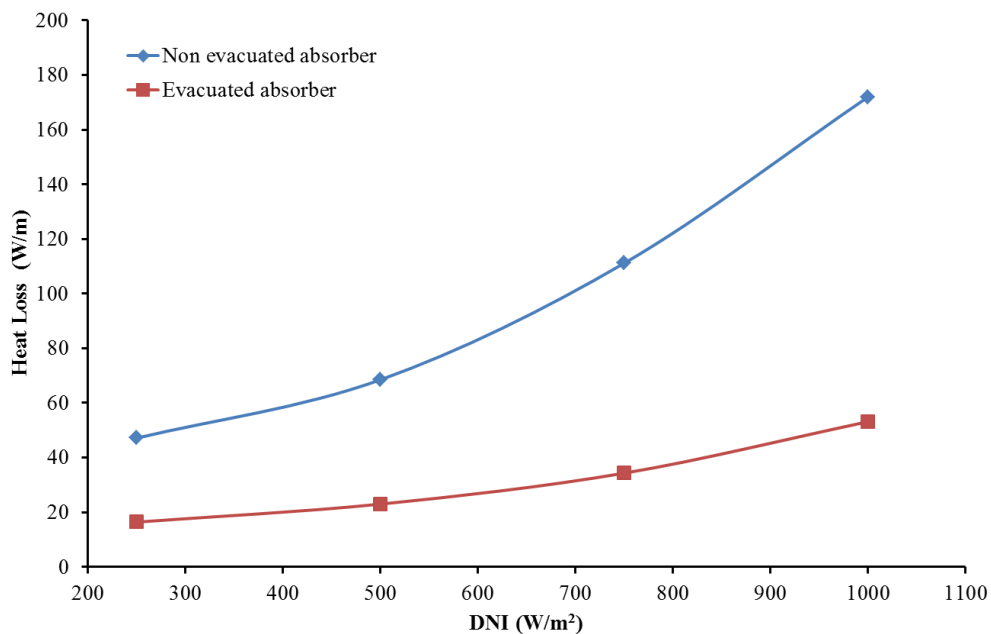


Fig. 4: Total heat loss for different DNI from the 2-stage receiver system

Figure 5 shows the convective and radiative heat losses for DNI ranging from 250W/m<sup>2</sup> to 1000W/m<sup>2</sup> for evacuated and non-evacuated annular region between the absorber and the glass tube. It is observed that the convection heat loss gets reduced by 40% under evacuated condition. Percentage of radiation heat loss varies between 28% and 57.5% from lower to higher flux conditions

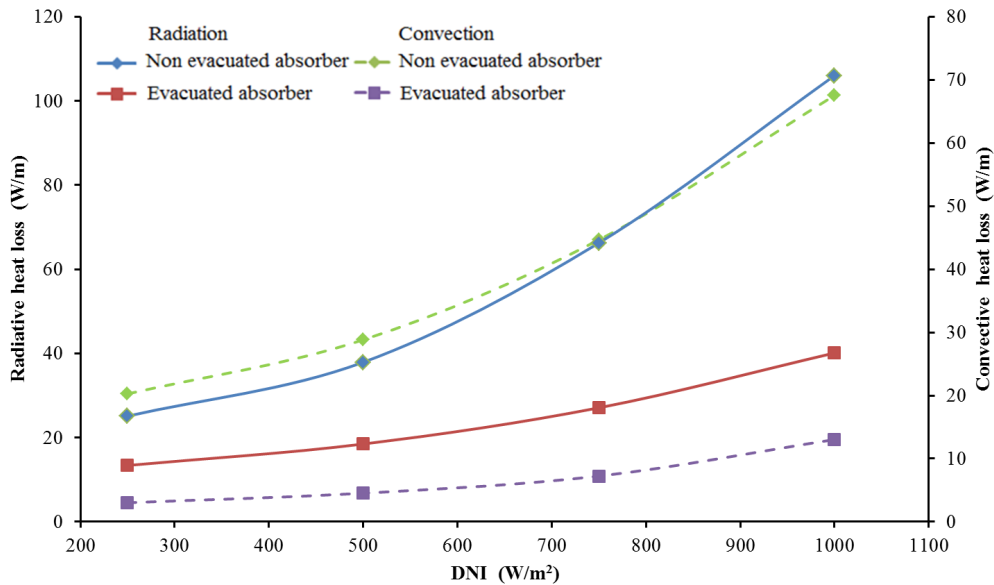


Fig. 5: Radiative and convective heat losses for different DNI

The individual components of heat loss, the radiative and the convective heat losses are studied. It is perceived that as the annular region is evacuated, the convective mode of heat transfer is minimized to a negligible amount and is shown in Fig. 5. When the residual gas in the gap is filled with air, the convective heat loss lies in the range of 30W/m to 100W/m for 250W/m<sup>2</sup> to 1000W/m<sup>2</sup>. When the tube is evacuated, the convective heat loss reduces from 3W/m to 15W/m while the radiative loss is about 13W/m to 40W/m. It is obvious that as the tube is evacuated, the convective component of the heat loss is completely negligible.

#### 4.2. Effect of gap between the absorber and the glass tube on the heat loss

Non-dimensionalization of the annular distance between the absorber and the glass tube is carried out by considering the ratio of the diameter of the absorber to the diameter of the protective glass. Total and the individual

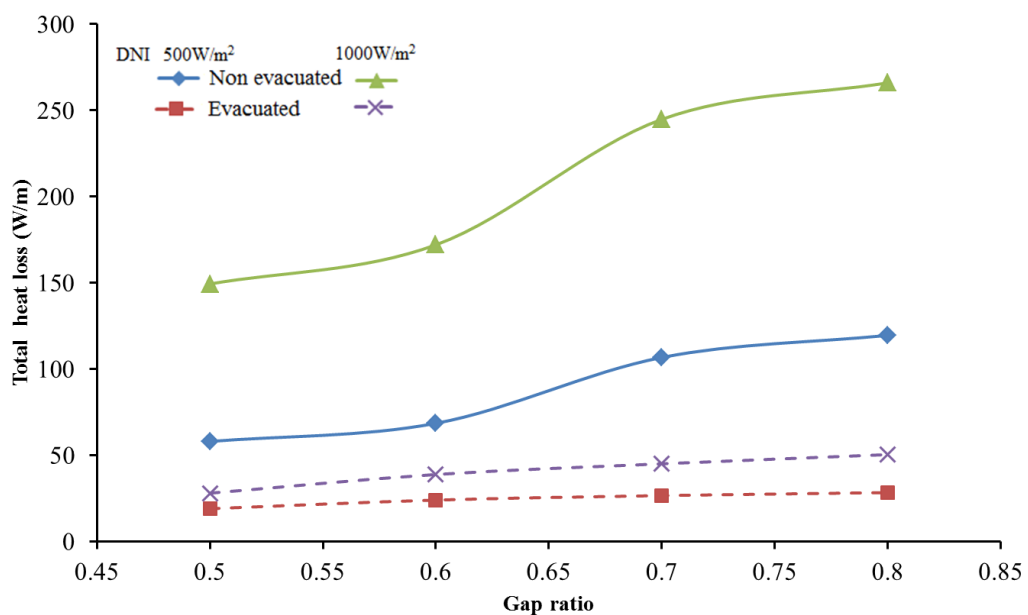


Fig. 6: Total heat losses for gap ratio between the absorber and the glass tube



components of heat transfer are studied. Variation in the heat loss for DNI of  $500\text{W/m}^2$  and  $1000\text{W/m}^2$  are investigated for both the evacuated and the non-evacuated conditions. Based on the commercial availability of SS absorber tube, the diameter of the absorber tube and the protective glass tube for the present study is chosen. Without compromising the diameter with the performance of the receiver system, it is observed from Fig. 6 that, the ratio of 0.6 has better performance and optimized annular region for less heat loss. When the tube is evacuated, the heat loss is observed to be constant for the range of gap ratio. The convective and the radiative heat loss components for the gap ratio between 0.5 and 0.8 for DNI of  $500\text{W/m}^2$  and  $1000\text{W/m}^2$  are shown in fig. 7 and fig. 8 respectively. When the tube is non-evacuated both the

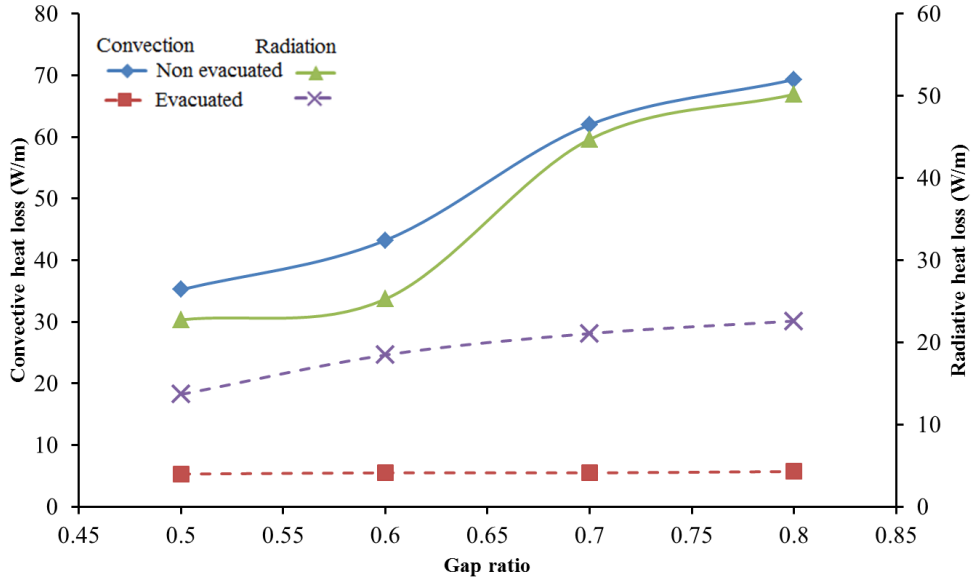


Fig. 7: Convective and radiative heat losses for different ratio of gap between the absorber and the glass tube for DNI of  $500\text{W/m}^2$

convective and the radiative components equally play a role in the heat loss. From Fig. 7, gap ratio of 0.5 to 0.6, heat loss of  $35\text{W/m}$  and  $22\text{W/m}$  on convective and radiative mode were observed. While at a higher ratio, convection and radiation heat loss exceed till  $69\text{W/m}$  and  $50\text{W/m}$  respectively. When the tube has vacuum, radiation component increases from  $13.67\text{W/m}$  to  $22.6\text{W/m}$  for the gap ratio from 0.5 to 0.8.

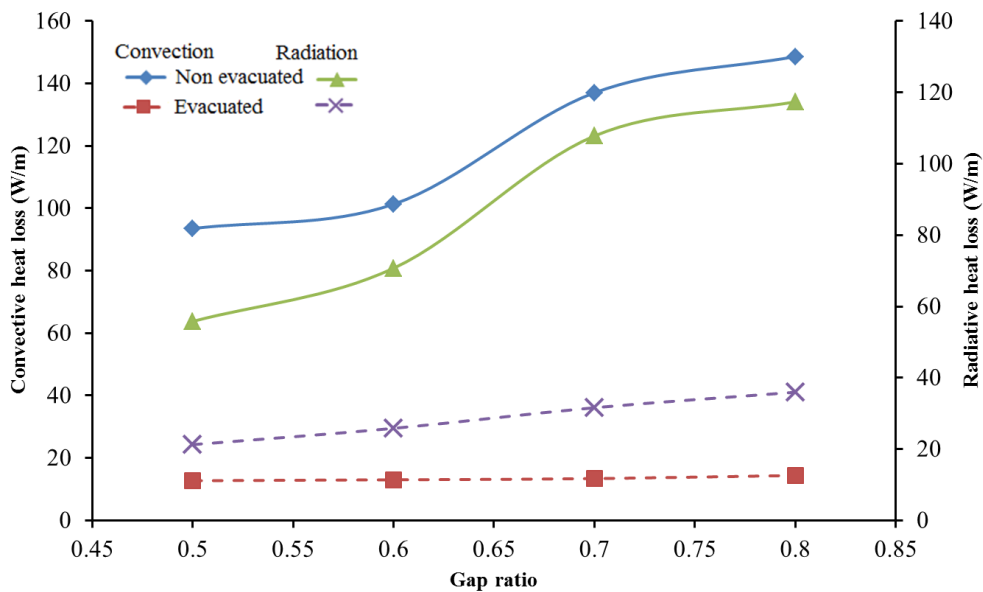


Fig. 8: Convective and radiative heat losses for different ratio of gap between the absorber and the glass tube for DNI of  $1000\text{W/m}^2$

The convective heat loss is at a constant level for different gap ratio. In Fig. 8, similar trend as of Fig. 7 is perceived. The convection and the radiation heat losses from the non-evacuated receiver increases by 57.5% and 58.5% and for evacuated conditions 36% and 59% respectively as the DNI increases from 500W/m<sup>2</sup> to 1000W/m<sup>2</sup> for the range of gap ratio.

## 5. Conclusion

A numerical study has been carried out to determine the heat loss from the 2-stage receiver system of the pilot plant in Vallipuram (12.65N, 79.74E), Tamil Nadu, India. Comprehensive analyses have been carried out to optimize the profile of the receiver system and then the thermal performance has been carried out. In the present work, the 2-stage receiver system is investigated when the absorber is under evacuated and non-evacuated conditions. A parametric study has been carried out by varying the DNI and the annular gap between the absorber and the protective glass. When the gap is filled with air, the heat loss varies from 47.14W/m to 172 W/m for 250W/m<sup>2</sup> to 1000W/m<sup>2</sup> respectively and when the region is evacuated, the percentage of heat loss is reduced from 16% to 70%. The convection and the radiation heat losses from the non-evacuated receiver increases by 57.5% and 58.5% and for evacuated conditions 36% and 59% respectively as the DNI increases from 500W/m<sup>2</sup> to 1000W/m<sup>2</sup> for the range of gap ratio.

## 6. References

- Balaji, S., Reddy, K.S., Sundararajan, T., 2016. Optical modelling and performance analysis of a solar LFR receiver system with parabolic and involute secondary reflectors. *Applied Energy* 179. doi:10.1016/j.apenergy.2016.07.082
- Chaitanya Prasad, G.S., Reddy, K.S., Sundararajan, T., 2017. Optimization of solar linear Fresnel reflector system with secondary concentrator for uniform flux distribution over absorber tube. *Solar Energy* 150, 1–12. doi:10.1016/j.solener.2017.04.026
- Guadamud, E., Oliva, A., Lehmkuhl, O., Rodriguez, I., González, I., 2015. Thermal Analysis of a Receiver for Linear Fresnel Reflectors. *Energy Procedia* 69, 405–414. doi:10.1016/j.egypro.2015.03.047
- Okafor, I.F., Dirker, J., Meyer, J.P., 2017. Influence of non-uniform heat flux distributions on the secondary flow, convective heat transfer and friction factors for a parabolic trough solar collector type absorber tube. *Renewable Energy* 108, 287–302. doi:10.1016/j.renene.2017.02.053
- Okafor, I.F., Dirker, J., Meyer, J.P., 2014. Influence of circumferential solar heat flux distribution on the heat transfer coefficients of linear Fresnel collector absorber tubes. *Solar Energy* 107, 381–397. doi:10.1016/j.solener.2014.05.011
- Reddy, K.S., Kumar, K.R., 2014. Estimation of convective and radiative heat losses from an inverted trapezoidal cavity receiver of solar linear Fresnel reflector system. *International Journal of Thermal Sciences* 80, 48–57. doi:10.1016/j.ijthermalsci.2014.01.022
- Sahoo, S.S., Singh, S., Banerjee, R., 2012. Analysis of heat losses from a trapezoidal cavity used for Linear Fresnel Reflector system. *Solar Energy* 86, 1313–1322. doi:10.1016/j.solener.2012.01.023
- Siegel, R., Howell, J., 2002. *Thermal Radiation Heat Transfer*, 4th Editio. ed. Taylor & Francis, New York.
- Singh, P.L., Sarviya, R.M., Bhagoria, J.L., 2010. Heat loss study of trapezoidal cavity absorbers for linear solar concentrating collector. *Energy Conversion and Management* 51, 329–337. doi:10.1016/j.enconman.2009.09.029
- Zou, B., Dong, J., Yao, Y., Jiang, Y., 2017. A detailed study on the optical performance of parabolic trough solar collectors with Monte Carlo Ray Tracing method based on theoretical analysis. *Solar Energy* 147, 189–201. doi:10.1016/j.solener.2017.01.055

## 7. Nomenclature

Quantity	Symbol	Unit
Area	$A$	m <sup>2</sup>
Heat loss	$\dot{Q}$	W/m
Temperature	$T$	K
Emissivity	$\varepsilon$	
Stefan-Boltzmann constant	$\sigma$	W m <sup>-2</sup> K <sup>-4</sup>
Density	$\rho$	Kgm <sup>-3</sup>